

X-ray spectra produced by a hot plasma containing cold clouds

Julien Malzac¹, Annalisa Celotti²

¹*Osservatorio Astronomico di Brera, via Brera, 28, 20121 Milan, Italy*

²*SISSA, via Beirut 2-4, 34014 Trieste, Italy*

Accepted, Received

ABSTRACT

We compute the hard X-ray spectra from a hot plasma pervaded by small cold dense clouds. The main cooling mechanism of the plasma is Compton cooling by the soft thermal emission from the clouds. We compute numerically the equilibrium temperature of the plasma together with the escaping spectrum. The spectrum depends mainly on the amount of cold clouds filling the hot phase. The clouds covering factor is constrained to be low in order to produce spectra similar to those observed in Seyfert galaxies and X-ray binaries, implying that an external reflector is required in order to reproduce the full range of observed reflection amplitudes. We also derive analytical estimates for the X-ray spectral slope and reflection amplitude using an escape probability formalism.

Key words: accretion, accretion discs – black hole physics – radiative transfer – gamma-rays: theory – galaxies: Seyfert – X-rays: general

1 INTRODUCTION

The physical conditions in the inner parts of the accretion flow surrounding a black hole are likely to be very chaotic. A situation that has been often considered in the literature is that of the so-called ‘cauldron’, where a soup formed by a hot plasma contains small grains constituted by small dense clouds of much colder matter (e.g. Guilbert & Rees 1988). Several works were devoted to explain how such a configuration could be physically realized and compute the spectrum emitted by the clouds for different cloud optical depths (see e.g. Rees 1987; Ferland & Rees 1988; Rees, Netzer & Ferland 1989; Celotti, Fabian & Rees 1992; Kuncic, Blackman & Rees 1996; Collin-Souffrin et al. 1996; Kuncic, Celotti & Rees 1997; Krolik 1998). In particular the main observable effect of optically thick cold clouds is the reprocessing into soft UV photons of the hard X-ray radiation produced in the hot phase by the Comptonisation process. This reprocessed emission is likely to contribute, at least partly, to the big blue bump observed in AGN. In addition, the presence of such clumps inside the hot plasma may also contribute to the formation of a reflection component (see e.g. Nandra & George 1994), responsible for the bump in the hard X-ray domain, commonly observed in Seyfert galaxies and galactic black hole candidates.

Most of the previous works on cloud models focused on the physics and radiative processes in the clouds themselves,

without taking into account the possible effects of the clouds on the characteristics of the hot phase. Indeed the soft radiation re-emitted by the cold material can constitute the main radiation field responsible for the Compton cooling of the hot gas. This in turn affects the temperature of the hot plasma, and thus the emitted X-ray Comptonised spectrum.

This feedback loop is identical to that found in accretion disc corona models (Haardt & Maraschi 1993). Similarly, the conditions at radiative equilibrium depend mainly on the cold matter distribution relative to the hot plasma. In this context, Malzac (2001) (hereafter M01) studied a geometry where the clouds are external to the hot Comptonising plasma and spherically distributed around it. The aim of the present work is to study the effects of the presence of cold optically thick clouds distributed *inside* the hot phase. As demonstrated below, the cooling by the cold clouds is then more efficient than in the case of an external reprocessor.

Under assumptions detailed in section 2, we use a numerical approach based on non-linear Monte-Carlo simulations, described in section 3, to compute the emitted spectra. These numerical results are found to be in agreement with analytical formulae, derived in section 4, giving the slope of the primary X-ray Comptonised spectrum Γ and the reflection amplitude R . The predictions of the model are then discussed and compared with the data in section 5.

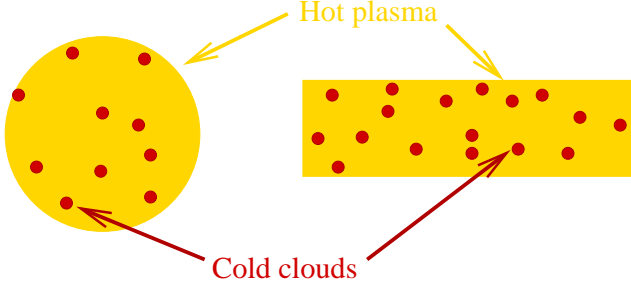


Figure 1. The hot plasma emitting the hard X- and soft γ -ray emission is pervaded by small lumps of cold dense matter. The geometry of the hot plasma could be close to spherical (left) or slab (right). The cold matter is assumed to be homogeneously distributed inside the plasma volume. The ambient high energy radiation which is intercepted by the cold clouds is partly reprocessed as low energy (UV, EUV) radiation and partly reflected in the X- and γ -ray energy domains. The system is assumed to be in radiative equilibrium.

2 MODEL ASSUMPTIONS AND PARAMETERS

The physical characteristics of the clouds are of prime importance for the emitted spectrum. If they are optically (Thomson) thin, and with a large covering fraction, partial transmission of the X-ray radiation across a cloud is likely to produce strong absorption features in the X-ray spectrum (e.g. Kuncic, Celotti & Rees 1997). On the other hand, if the clouds are optically thick and highly absorbing they do not produce, independent of their covering fraction, strong apparent absorption features, as indeed observed (Nandra & George 1994).

For this reason in this analysis we will consider the case of optically thick clouds with zero transmission, which corresponds to typical column densities $\gtrsim 10^{25} \text{ cm}^{-2}$. We assume that the individual cold clouds are much smaller than the characteristic size of the region occupied by the hot plasma: if the emitting region has a typical dimension H , the typical cloud size is of order ϵH with $\epsilon \lesssim 10^{-2}$ *. This constrains the cloud hydrogen density to be large, larger than $(\sigma_T \epsilon H)^{-1}$. This limit writes $n_H \gtrsim 10^{12} \text{ cm}^{-3}$ in the case of Seyfert galaxies (AGN, with $H \simeq 10^{15} H_{15} \text{ cm}$), and $n_H \gtrsim 10^{20} \text{ cm}^{-3}$ in the case of galactic black holes (GBH, where $H \simeq 10^7 H_7 \text{ cm}$). Such large densities in turn constrain the ionization parameter to be relatively low ($\xi < 10^3$ for a $10^{45} \text{ erg s}^{-1}$ luminosity AGN, and $\xi < 10^2$ for a $10^{36} \text{ erg s}^{-1}$ GBH) and thus the possible effects of ionization are likely to be weak (Życki et al. 1994). In our calculations we will then assume that the clouds are neutral.

We will consider a system in radiative equilibrium. The effective temperature of the clouds kT_{bb} can be simply estimated. Assuming that the flux is uniform inside a spherical hot phase of bolometric luminosity L , a cloud surface element will receive a flux $F = L/(4\pi H^2)$. If the clouds are dense enough this flux is fully absorbed and re-radiated as a quasi-blackbody (e.g. Ferland & Rees 1988) and the Stefan-Boltzmann’s law gives well known characteristic energies:

* For simplicity we will assume spherical clumps, although filamentary or sheet-like geometries might be also appropriate.

$$kT_{\text{bb}} \simeq 2.97 \frac{L_{45}^{1/4}}{H_{15}^{1/2}} \text{eV} \simeq 167 \frac{L_{36}^{1/4}}{H_7^{1/2}} \text{eV}, \quad (1)$$

where L_{45} and L_{36} are the bolometric luminosity expressed respectively in 10^{45} and $10^{36} \text{ erg s}^{-1}$ units. We will assume that the radiation reprocessed by the clouds is the only source of soft seed photons.

As we are focusing on the spectral signatures of this two phase medium and as they do not constrain – as already mentioned – the physical status of the clouds (as long as they are optically thick and dense enough to maintain a low temperature), the clumps might exist with a large range of conditions. Nonetheless the range of parameters considered (in dimension and density) are consistent with assuming that the gas reaches radiative equilibrium (i.e. the cooling timescales are shorter than the dynamical one) and pressure equilibrium (with a size ϵH small enough to reach it in a dynamical timescale).

In general if neutral clouds are confined by a hot ionized environment the thermal pressure balance can be written in terms of the cloud Thomson optical depth $\tau = n_H \sigma_T \epsilon H$:

$$\tau \sim 2\epsilon \tau_T T_e / T_{\text{bb}}. \quad (2)$$

For typical observationally inferred values of $\tau_T = 1$ and $kT_e = 100 \text{ keV}$, and using the expressions (1) for the temperature of the cold clouds, equation (2) reads:

$$\tau \sim 64\epsilon_{-2} \frac{H_{15}^{1/2}}{L_{45}^{1/4}} \sim 12\epsilon_{-2} \frac{H_7^{1/2}}{L_{36}^{1/4}}, \quad (3)$$

where $\epsilon = 10^{-2} \epsilon_{-2}$. We note however that this simple estimate does not consider the possibility of a two temperature plasma and the consequent effects of hot ions on the thermal balance (see Zdziarski 1998; Spruit & Haardt 2000; Deufel & Spruit 2000).

Thus the thick clouds considered here can be confined by the hot phase, but in any case thicker clouds may exist and be e.g. magnetically confined (for more details see e.g. Kuncic, Blackman & Rees 1996). Note that the clumps do not need to survive for longer than their cooling time provided they can be continuously replaced.

Let us now consider the spectrum produced in these environment. The three main parameters controlling the resulting X-/ γ -ray spectral shape are the following:

(i) The amount of cold clouds pervading the hot plasma. Since we consider small scale clumps we can quantify the amount of cold matter by using an effective “cloud” optical depth τ_B , such that a photon crossing the hot plasma has a probability $1 - \exp(-\tau_B)$ of intercepting a cloud. τ_B may be thus defined using a cross section formalism, considering an individual cloud as a particle:

$$\tau_B = \frac{N}{V} \langle A \rangle H \quad (4)$$

where V is the plasma volume, N is the total number of cold clouds, $\langle A \rangle$ is the average geometric cross section of each cloud. For spherical clouds pervading a spherical plasma, τ_B can be written explicitly in term of the number and size of the clouds:

$$\tau_B = \frac{3N\epsilon^2}{4} \quad (5)$$

(ii) The Thomson optical depth τ_T of the hot plasma.

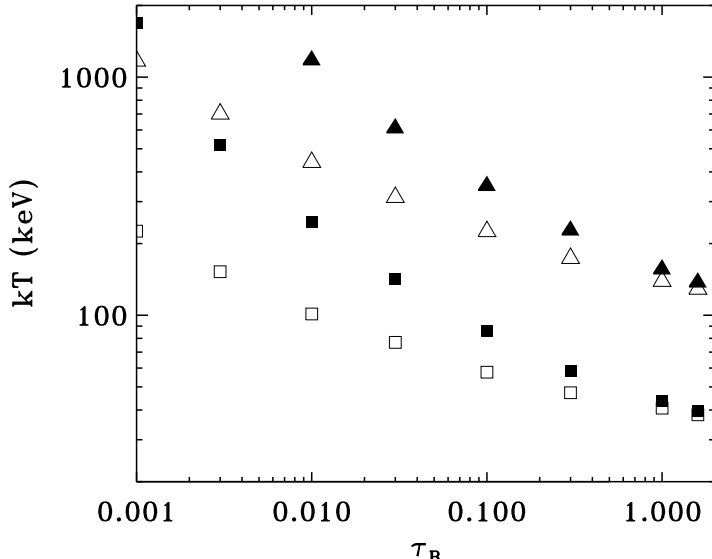


Figure 3. The volume averaged electron temperature versus τ_B . Filled and open symbols correspond to $kT_{\text{bb}} = 150$ eV (GBHs) and $kT_{\text{bb}} = 5$ eV (AGN), respectively. Squares and triangles refer to the cases $\tau_T = 2$ and $\tau_T = 0.5$.

(iii) The characteristic energy of the soft photons emitted by the clouds. We assume a blackbody spectrum with a fixed temperature kT_{bb} . As the radiative equilibrium is not extremely sensitive to the value of kT_{bb} , we will fix $kT_{\text{bb}} = 5$ eV and $kT_{\text{bb}} = 150$ eV as typical values for Seyfert galaxies and GBH sources, respectively, as from equation (1).

As said before, the amount of cold matter and its distribution with respect to the hot plasma are of prime importance. On the other hand, the actual geometry of the emitting region has little effects on the emitted spectrum. We studied both the spherical and infinite slab geometries illustrated in Fig. 1. As the results were qualitatively similar for both geometries, in the following we consider the spherical case only.

3 NUMERICAL APPROACH

In order to estimate the resulting physical parameters and spectra we use the Monte-Carlo code of Malzac & Jourdain (2000) which is based on the Non-Linear Monte-Carlo method (NLMC) proposed by Stern (Stern 1985; Stern et al. 1995). We consider a spherical geometry. The sphere is divided in 5 shells with equal thicknesses and is assumed to have a uniform density. Both τ_B and τ_T are defined along the radius H of the sphere.

In the hot phase, the simulations are fully non-linear: both photons and electrons are followed using the Large Particles (LP) formalism described in Stern et al. (1995). This enables the equilibrium temperature to be computed in each zone according to the local energy balance heating = Compton cooling.

The interaction between a photon and a cloud is dealt as a regular Monte-Carlo interaction between two particles. However, as the cold clouds structure is assumed to be unaffected by the radiation field, the clouds themselves are not followed. As the clouds are small and homogeneously distributed, τ_B is simply the reaction rate for 1 photon, with

time expressed in units of the light crossing time H/c of the medium. When a LP photon interacts with a cloud, it is assumed to enter a semi-infinite slab medium with standard abundances and neutral matter (Morrison & Mc Cammon 1983). The linear Monte-Carlo code of Malzac et al. (1998), is then used to track the path and the energy changes of the LP photon in this medium, until it is either absorbed or escapes from the cold matter slab. As long as the clouds are optically thick, the reflection spectrum on a cloud does not differ much from slab reflection (Nandra & George 1994). A more detailed modeling of the reflection component would rely on a specific cloud geometry which is essentially unknown.

The energy deposited in the cloud is re-injected in the hot phase in the form of thermal soft photons LP. Both the reflected and reprocessed LP have a direction of propagation drawn from an isotropic distribution.

4 ANALYTICAL ESTIMATES OF R AND Γ

There are two parameters generally used to phenomenologically describe the X-ray spectral properties of accreting black hole sources, namely the amplitude R of the reflection component with respect to the primary continuum and the photon spectral index Γ of the power-law shaped primary component (see Malzac, Beloborodov & Poutanen 2001, MBP hereafter).

These parameters were determined from the numerical simulations in a way similar to that described in MBP. The reflection was estimated by computing the flux ratio between our simulated reflection, and the angle-averaged slab-reflection produced by a source having the same primary spectrum as the simulated one.

However, using the simple escape probability formalism described in the following, it is also possible to independently derive analytical estimates for R and Γ , as follows.

A power L_h is deposited in the plasma as heating and escapes the system as three different kinds of radiation:

$$L_h = L_{\text{uv}} + L_x + L_R, \quad (6)$$

respectively the UV/soft X-ray reprocessed luminosity, the X-ray (Comptonized) luminosity, and the reflected luminosity. Let U_h be the total radiative energy inside the hot plasma. With similar notations as in equation (6) we have:

$$U_h = U_{\text{uv}} + U_x + U_R. \quad (7)$$

The escaping luminosity is related to the internal energy through the escape probability (Lightman & Zdziarski 1987):

$$\dot{P}_h = (L_h/U_h)(H/c), \quad (8)$$

which depends on the geometry, sources distribution, optical depth and energy. We consistently indicate as $\dot{P}_x, \dot{P}_s, \dot{P}_R$ the escape probability for Comptonised, soft and reflected radiation and will use the analytical approximation to \dot{P} given in the Appendix (equation (20)).

Let us now estimate the three different luminosities.

The soft luminosity in the hot phase is produced by the clouds through absorption and reprocessing of the Comptonized and reflected radiation and disappears through es-

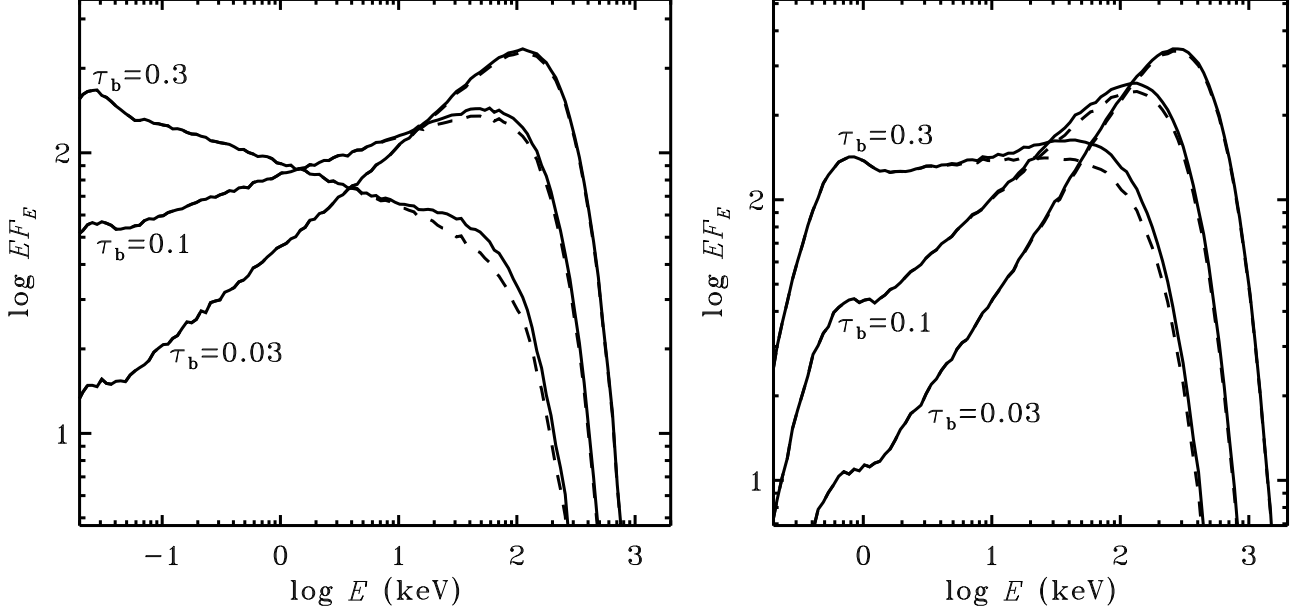


Figure 2. Examples of spectra produced by the lumpy model as a function of the indicated values of τ_B . The dashed lines show the resulting spectra without the reflection component. The left panel corresponds to the case of AGN ($kT_{bb} = 5$ eV). The right panel corresponds to GBHs ($kT_{bb} = 150$ eV). The spectra (in arbitrary flux units) are angle-averaged and normalized to the same total luminosity. The plasma Thomson optical depth is $\tau_T = 2$.

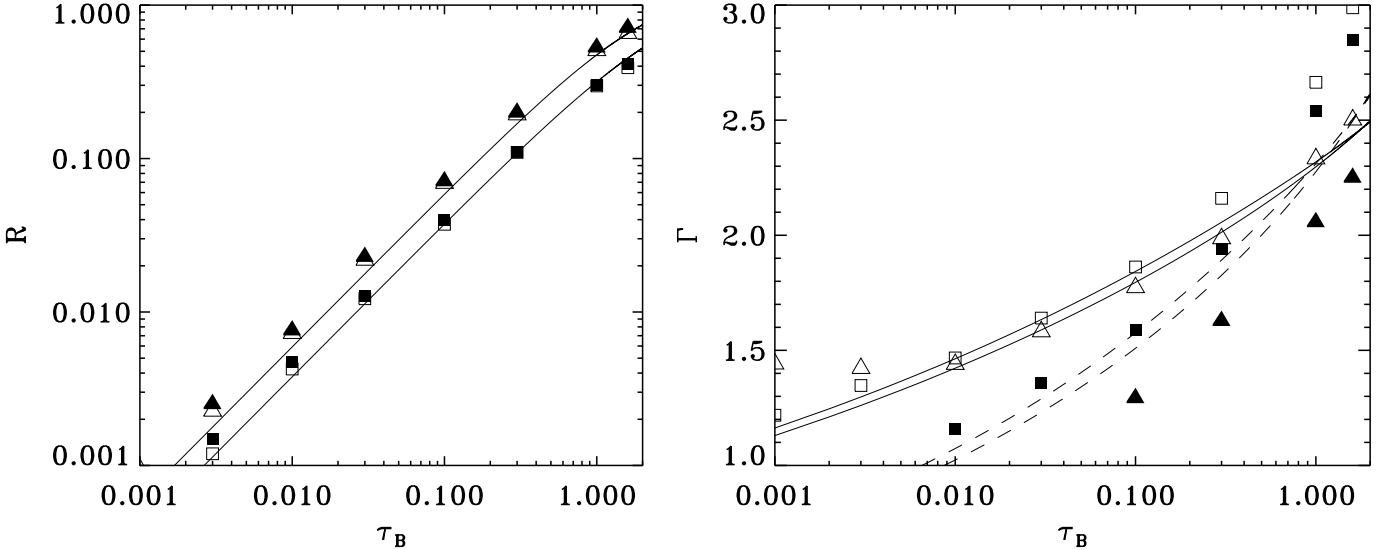


Figure 4. Angle averaged reflection (left-hand panel) and spectral index (right-hand panel) versus τ_B . Filled and open symbols correspond to $kT_{bb} = 150$ eV (GBHs) and $kT_{bb} = 5$ eV (AGN), respectively. Squares and triangles show the cases $\tau_T = 2$ and $\tau_T = 0.5$. In both panels, the curves represent the analytical approximation to the numerical results (see text). The solid lines stand for $kT_{bb} = 5$ eV (AGN), the dashed lines for $kT_{bb} = 150$ eV.

cape or Comptonisation. Thus, the radiative equilibrium balance for U_{uv} reads:

$$(\dot{P}_s + \tau_T)U_{uv} = \tau_B(1-a)U_x + \tau_B(1-a_R)U_R, \quad (9)$$

where a and a_R are the clouds energy and angle integrated albedo for a Comptonised and a reflection spectrum, respectively. For neutral matter the typical values are $a \sim 0.1$ (Magdziarz & Zdziarski 1995; MBP) and $a_R \sim 0.4$ (Malzac 2001).

Similarly, the reflected radiation is formed through reflection of the Comptonised and reflected radiation on the

clouds, and disappears via escape, Comptonisation in the hot plasma and absorption by the clouds:

$$(\dot{P}_R + \tau_T + \tau_B(1-a_R))U_R = \tau_B a U_x. \quad (10)$$

The fraction of the internal energy in the form of Comptonised radiation has as main source the power dissipated in the hot plasma but also the Comptonised soft and reflected radiation; the sink term is due to escape, absorption and reflection by the clouds:

$$(\dot{P}_x + \tau_B)U_x = L_h H/c + \tau_T U_{uv} + \tau_T U_R. \quad (11)$$

Excluding the reflection component, the total luminosity sinking out of the hot phase either through escape or interaction with the clouds is:

$$L = (\dot{P}_s + \tau_B)U_x + (\dot{P}_s + \tau_B)U_{uv}, \quad (12)$$

while the soft luminosity entering the hot phase (coming from the clouds) is given by equation (9):

$$L_s = (\dot{P}_x + \tau_T + \tau_B)U_{uv}. \quad (13)$$

Therefore combining equations (12) and (13) with equations (9) and (10) provides an estimate for the amplification factor $A \equiv L/L_s$:

$$A = \frac{(\dot{P}_s + \tau_B)\tau_B + (\dot{P}_x + \tau_B)(\dot{P}_s + \tau_T)g}{\tau_B(\dot{P}_s + \tau_T + \tau_B)}, \quad (14)$$

where the factor g is given by:

$$g = \frac{\dot{P}_R + \tau_T + \tau_B(1 - a_R)}{(\dot{P}_R + \tau_T)(1 - a) + \tau_B(1 - a_R)}. \quad (15)$$

Note that at first order $g \simeq 1$ and $\dot{P}_x \simeq \dot{P}_s$ and thus:

$$A \sim 1 + \dot{P}_x/\tau_B. \quad (16)$$

Finally the amplification factor is clearly directly related to the photon index Γ , which can therefore be expressed – using the phenomenological formula given by Beloborodov (1999) – as

$$\Gamma = 2.33(A - 1)^{-1/\delta}, \quad (17)$$

where the parameter $\delta = 1/10$ for AGN and $1/6$ for GBHs.

In addition equation (10) provides an estimate for the second parameter, the reflection coefficient:

$$R \sim \frac{L_R}{aL_x} \sim \frac{\dot{P}_R}{\dot{P}_x} \frac{\tau_B}{\dot{P}_R + \tau_T + \tau_B(1 - a_R)}. \quad (18)$$

This formula corresponds to an angle averaged reference slab-reflection spectrum. Actually, the reflection coefficient also depends on the assumed inclination angle for the infinite slab model (see e.g. PEXRAV model in XSPEC, Magdziarz & Zdziarski 1995). Equation (18) could be corrected for this, for example by dividing it by the angular factor given by equation 2 of Ghisellini, Haardt & Matt (1994). However, for the relatively low inclination angles usually assumed in spectral fits, the correction is small and, for simplicity, we will neglect it.

5 RESULTS

Figure 2 shows some of the simulated spectra for different values of τ_B . The radiative cooling from the clouds appears to be extremely efficient and starts being effective for values of τ_B as low as a few $\times 10^{-2}$. At fixed τ_T and T_{bb} , increasing τ_B increases the cooling of the plasma (because of the enhancement of the reprocessing and the subsequent increase of the soft radiation field) and therefore decreases its temperature (see below). This affects the shape of the emitted spectrum which becomes softer and cuts off at lower energies. Note that for the same set of parameters the spectra of GBHs (right panel of the figure) are harder than the AGNs ones (left panel) due to the larger energy domain where the luminosity can be released in the latter objects

(see e.g. MBP). The spectra shown are rather similar to what is observed in Seyfert galaxies and Galactic black hole candidates in their hard state (see e.g. Zdziarski et al. 1997, Poutanen 1998).

The dependence of the hot plasma temperature on τ_B is illustrated more precisely by Fig. 3. As just said the temperature is generally lower in AGNs (for the same τ_B) and it is higher for lower Thomson optical depths. While these are general features (see e.g. MBP) of the self-regulated Compton emission generally invoked by the two-phase models (Haardt & Maraschi 1993), note that in our case the product $T_e\tau_T$ is *not* expected to be constant at fixed τ_B since here the Compton parameter depends also slightly on τ_T (see Section 4).

The observed range of temperatures – say 50-200 keV – inferred from observations of the high energy cut off in Seyfert galaxies and GBHs can be reproduced for τ_B in the range 10^{-2} –1, depending also widely on τ_T . In the optically thick case larger values of τ_B may induce very low temperatures.

A second observable parameter is the index of the (primary) X-ray spectrum. Fig. 4 shows the evolution of the 2–10 keV spectral slope for increasing τ_B : as expected the spectrum softens very quickly for larger τ_B . One can see that the range of spectral slopes observed in Seyfert galaxies and GBH in the hard state (approximately the range 1.4–2.2) can be achieved for τ_B roughly in the interval 10^{-3} –1 (larger τ_B clearly lead to a too soft spectrum). Note that although such interval is rather large, the dependence on τ_B is quite steep especially in the GBH case.

Finally let us examine the results on the intensity of the reflection component, shown in Fig. 4 (left-hand panel). This immediately reveals that the inferred values of R are rather low, even when τ_B approaches unity, and in general significantly lower than observed. According to equation (18), R values of order of unity can be achieved in the limit of large τ_B . However, this corresponds to very large (and unobserved) Γ , as discussed in the next section.

As shown in the same Fig. 4, we also stress here that there is good agreement between the numerical results and the analytical estimates of R and Γ derived in section 4. Concerning Γ , we note however a significant discrepancy for the GBH optically thin case, for which the simulations give a much harder spectrum than the analytical estimates. Indeed, in this case the first Compton scattering order falls in the 2–10 keV range. This forms a bump making the spectrum locally harder in the energy range used to estimate Γ , and with a break at higher energy. This (unobserved) radiative transfer effect is due to the low optical depth ($\tau_T=0.5$) considered. A part from this the main discrepancies appear in the optically thick case and at large τ_B (corresponding to Γ outside the observed range) arising because in this interval of parameters associated with low temperatures, equation (17), which is formally valid for a spherical plasma with temperature in the range 50–100 keV, does not provide a good approximation to the Γ vs A relation anymore.

6 CONCLUSIONS

From the computation of the spectra expected in a scenario where cold reflecting and reprocessing gas is embedded in

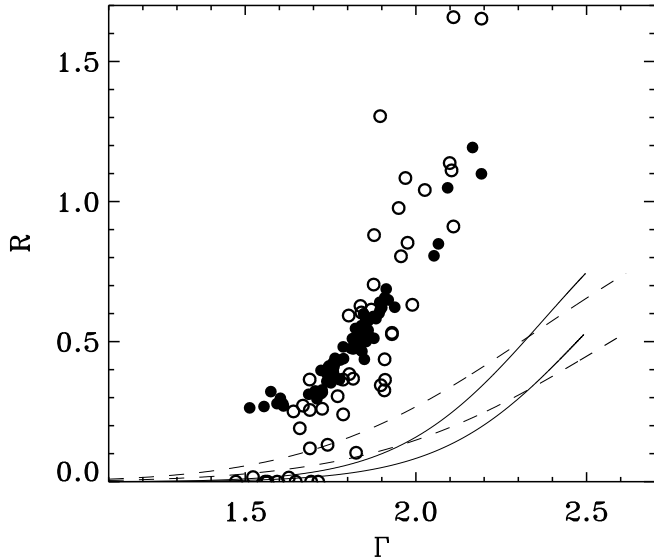


Figure 5. The circles show data in the R - Γ plane corresponding to the sample of Seyfert galaxies (open circles) of Zdziarski et al. (1999) and the sample of galactic black holes (filled circles) presented in Gilfanov et al. (2000). The lines refer to the analytical model predictions: along these lines τ_B is varied at constant τ_T . Dashed and solid lines correspond to $kT_{bb}=150$ eV (GBHs) and $kT_{bb}=5$ eV (AGN) respectively. For both types of sources, the model predictions are plotted for $\tau_T=0.5$ (upper curves), and $\tau_T=2$ (lower curves), τ_B covers the range 0–2 along the curves.

a coronal hot plasma we have inferred constraints on the distribution of such cold gas. In fact, having assumed that the gas can be described as small optically thick clouds, the main parameter regulating the amount of reprocessing (in turn responsible for the Compton cooling) and reflection is the cloud optical depth τ_B , which quantifies the covering factor of the cold component.

This has to be relatively low. In fact, the observed range of spectral slopes constrains $\tau_B < 1$. This limit however forbids to produce simultaneously a reflection amplitude larger than ~ 0.3 . The situation is even more critical since $R \sim 0.3$ is predicted only for the softest sources which observationally appear to show the largest reflection amplitude ($R \gtrsim 1$), as shown in Fig. 5.

Thus, in order to reproduce the spectral characteristics of numerous objects (both Seyfert galaxies and GBH sources) with significant reflection the model requires an additional reflecting medium which does not contribute to the soft photon field, such as e.g. a cold outer accretion disc, reflection on a torus in the case of Seyfert galaxies or on the companion star in the case of X-ray binaries.

The reported correlation between R and Γ (shown in Fig. 5) is generally interpreted as being due to plasma cooling on soft photons emitted by the same medium that gives rise to the reflection component (see Zdziarski et al. 1999; Gilfanov et al. 2000). If the R - Γ correlation were indicative of a common medium for soft photon creation and reflection, such a medium cannot be provided by cold matter mixed together with the hot phase, and another reflector should contribute to, and even dominate the radiative cooling of the hot plasma.

A related problem is the observed correlation between

the degree of relativistic broadening of the Fe line with Γ (Gilfanov et al. 2000 for black hole binaries, Lubiński & Zdziarski 2001 for Seyferts, see however Yaqoob et al. 2002). In the context of the present model this correlation would suggest that the overall cloud distribution is not homogeneous. The changes in the amount of cold material pervading the hot plasma should be stronger in the innermost parts of the accretion flow where the relativistic broadening is important. However, since the reflection amplitude produced by the cold clump is weaker than observed, this requires that the bulk of the line would be emitted by the cold clouds while the reflection would come mainly from an external reflector.

Thus, the origin of both soft photons and reflection are unlikely to be matter mixed inside the hot Comptonising plasma. In the framework of the cloud models this suggests that the cold clouds should be essentially external to the hot Comptonising plasma. Then the radiative cooling is much less efficient and the reflection component may be larger. Variations in the covering factor and the distribution of the clouds may even produce a correlation between R and Γ (as e.g. in the spherical case considered by M01).

These conclusions should be however tempered by the fact that, in Seyfert galaxies, the R - Γ correlation is still a controversial matter on several grounds. Indeed, the measurement of the reflection amplitude R suffers from large uncertainties. In particular, it appears that the R values derived from spectral fits are very sensitive to the modelling of the primary spectrum (see e.g. Petrucci et al. 2001; Perola et al. 2002; Malzac & Petrucci 2002) as well as to the eventual presence of a secondary components such as a soft excess (Matt 2001). Possible effects such as ionization of the reflecting material, eventual relativistic smearing, Comptonisation of the reflected component may all affect the R values derived from the neutral slab reflection model generally used (PEXRAV). We also note that in NGC 5506, Lamer, Uttley & McHardy (2000) find an anti-correlation between R and Γ .

Also, even if the correlation is real, its interpretation could be different. Indeed, following Nandra et al. (2000), Malzac & Petrucci (2001, 2002) show that at least part of the observed correlation could be understood in term of the effects of time-delays between the fluctuations of the primary emission and the response of a large-scale distant reflector (e.g a torus). Obviously, because of the time-scales involved, this interpretation cannot be valid for black-hole binaries. On the other hand, in Seyfert galaxies, it is supported by spectral and variability studies indicating that, in several sources, an important fraction of the reflected features is produced at large distances from the central engine (e.g. Chiang et al. 2000 for NGC 5548; Matt et al. 2001 and Lamer et al. 2000, for NGC 5506; Done, Madejski & Życki 2000 for IC4329a, Papadakis et al. 2002, for a sample of sources). In a context where the reflection features would be produced mainly on distant material, the “cauldron” scenario considered here would remain a viable possibility.

Future observational studies of the R - Γ relation in samples of sources as well as in individual objects should clarify this point.

ACKNOWLEDGMENTS

JM acknowledges grants from the Italian MURST (COFIN98-02-15-41) and the European Commission (contract number ERBFMRX-CT98-0195, TMR network "Accretion onto black holes, compact stars and protostars"). AC acknowledges the MUIR for fundings. We thank Andrzej Zdziarski and Marat Gilfanov who provided the data used in this work.

REFERENCES

Beloborodov A. M., 1999, in Poutanen J., Svensson R., eds, ASP Conf. Series Vol. 161, High Energy Processes in Accreting Black Holes. Astron. Soc. Pac., San Francisco, p. 295
 Celotti A., Fabian A.C., Rees M.J., 1992, MNRAS, 255, 419
 Chiang J., Reynolds C.S., Blaes O.M., Nowak M.A., Murray N., Madejski G., Marshall H.L., Magdziarz P., 2000, ApJ, 528, 292
 Collin-Souffrin S., Czerny B., Dumont A.-M., Zycki P. T., 1996, A&A, 314, 393
 Deufel B., Spruit H.C., 2000, A&A, 362, 1
 Done C., Madejski G.M., Zycki P.T., 2000, ApJ, 536, 213
 Ferland, G.J., Rees, M.J., 1988, ApJ, 332, 141
 George I.M., Fabian A.C., 1991, MNRAS, 249, 352
 Ghisellini G., Haardt F., Matt G., 1994, MNRAS, 267, 743
 Gilfanov M., Churazov E., Revnivtsev M., 2000, in Proc. 5th CAS/MPG Workshop on High Energy Astrophysics, ed. G. Zhao et al. (Beijing: China Sci. Techn. Press), 114, (astro-ph/0002415)
 Guilbert P.W., Rees M.J., 1988, MNRAS, 233, 475
 Haardt F., Maraschi L., 1993, ApJ, 413, 507
 Kuncic Z., Blackman E.G., Rees M.J., 1996, MNRAS, 283, 1322
 Kuncic Z., Celotti A., Rees M.J., 1997, MNRAS, 284, 717
 Krolik J.H., 1998, MNRAS, 498, L13
 Lamer G., Uttley P., McHardy I.M., MNRAS, 2000, 319, 949
 Lightman A.P., Zdziarski A.A., 1987, ApJ, 319, 643
 Magdziarz P., Zdziarski A. A., 1995, MNRAS, 273, 837
 Matt G., 2001, in "X-Ray Astronomy, Stellar Endpoints, AGN, and the Diffuse X-ray Background, Bologna, Italy 1999", Eds N.E. White, G. Malaguti, G.G.C. Palumbo, AIP conference proceedings 599, 209, (astro-ph/0007105)
 Matt G., Guainazzi M., Perola G.C., Fiore F., Nicastro F., Cappi M., Piro L., 2001, A&A, 377, L31
 Malzac J., Jourdain E., Petrucci P., Henri G., 1998, A&A, 336, 807
 Malzac J., Jourdain E., 2000, A&A, 359, 843
 Malzac J., 2001, MNRAS, 325, 1625
 Malzac J., Beloborodov A., Poutanen J., 2001, MNRAS, 326, 417
 Malzac J., Petrucci P.O., 2001, Proceedings of the "Workshop on X-ray emission from accretion onto black hole" 20-23 June 2001, www.pha.jhu.edu/groups/astro/workshop2001/papers/
 Malzac J., Petrucci P.O., 2002, MNRAS, submitted
 Morrison R., McCammon D., 1983, ApJ, 270, 119
 Nandra K., George I.M., 1994, MNRAS, 267, 974
 Nandra K., Le T., George I.M., Edelson R.A., Mushotski R.F., Peterson B.F., Turner T.J., 2000, ApJ, 544, 734.
 Papadakis I.E., Petrucci P.O., Maraschi L., McHardy I.M., Uttley P., 2002, ApJ, in press (astro-ph/0202498)
 Perola G.C. et al., 2002, A&A, submitted
 Petrucci P.O. et al. 2001, ApJ, 556, 716
 Poutanen J., 1998, in Abramowicz M. A., Björnsson G., Pringle J., eds, Theory of Black Hole Accretion Disks. Cambridge Univ. Press, Cambridge, p. 100
 Rees, M.J., 1987, MNRAS, 228, P47
 Rees, M.J., Netzer, H., Ferland, G.J., 1989, MNRAS, 347, 640

Spruit H. C., Haardt F., 2000, MNRAS, 315, 751
 Stern B. E., 1985, SvA, 29, 306
 Stern B., Begelman M.C., Sikora M., Svensson R., 1995, MNRAS, 272, 291
 Yaqoob T, Padmanabhan U., Dotani T., Nandra K., 2002, ApJ, in press, (astro-ph/0112318)
 Zdziarski A. A., 1998, MNRAS, 296, L51
 Zdziarski A. A., Lubiński P., Smith D. A., 1999, MNRAS, 303, L11 (ZLS99)
 Zdziarski A. A., Johnson W. N., Poutanen J., Magdziarz P., Gierliński M., 1997, in Winkler C., Courvoisier T. J.-L., Durouchoux Ph., eds, Proc. 2nd INTEGRAL Workshop, The Transparent Universe, ESA SP-382. ESA, Noordwijk, p. 373
 Zycki P. T., Krolik J. H., Zdziarski A. A., Kallman T. R., 1994, ApJ, 437, 597

APPENDIX: FITTING FORMULAE FOR THE ESCAPE PROBABILITY

Let us consider a medium where both scattering and absorption of radiation are effective, with τ_d the total optical depth of the medium for the scattering process and τ_a for absorption. Assume one injects instantaneously in the volume a number of photons according to a given spatial distribution. The photons can disappear from the medium either by real escape (i.e. by crossing the volume boundaries) or by absorption. Let f be the distribution of the photons at their disappearance time, and E the fraction of photons that truly escape the medium (i.e. not absorbed). Then, from the definition of the escape probability given by equation (8), it is straightforward to show that:

$$\frac{1}{\dot{P}} = \frac{1}{E} \int_0^{+\infty} dt \left(1 - \int_0^t f(t') dt' \right) \quad (19)$$

Using a standard Monte-Carlo method, we estimated E and the f function for different geometries and source distributions. In these calculations the scattering process was assumed isotropic and the distribution of scatterers and absorbers was homogeneous. We then computed numerically \dot{P} and searched for analytical formulae giving a reasonable representation of the numerical results in the range $\tau_d < 10$ and $\tau_a < 10$. The expressions given below agree within 5% with our numerical results. For slab and sphere geometries, the optical depths τ_a and τ_d are defined along the full height of the slab and the radius of the sphere, respectively. For a spherical geometry and uniform isotropic injection:

$$\frac{1}{\dot{P}} = 0.75 \left[1 + \frac{0.25\tau_d}{1 + 0.49\tau_a(1 + 0.1\tau_d)} \right] (1 + 2.28\tau_a)^{0.16}. \quad (20)$$

In the limit $\tau_a=0$ this formula reduces to that proposed by Stern et al. (1995).

For a spherical geometry and central isotropic injection:

$$\frac{1}{\dot{P}} = \left\{ 1 + 0.45\tau_d \left[1 + 3.384 \cdot 10^{-3} \tau_a^{1.168} \exp\{3.3(1.09 - 0.10887\tau_a)(10. - \tau_d)^{8.5 \cdot 10^{-3}} + 0.2999\tau_a + (0.346 + 0.1\tau_d)\tau_d^{0.681}\} \right] \right\} \frac{\exp(0.944\tau_a + 1.32 \cdot 10^{-3}\tau_a^2)}{1 + 0.56\tau_a}. \quad (21)$$

For an infinite slab geometry and homogeneous and isotropic source function:

$$\frac{1}{P} = 1 + 0.392 \left(\frac{183.7\tau_a}{1 + 183.6\tau_a} \right)^{533} + \frac{\tau_d/3}{(1 + 0.08\tau_d^{0.57})(1 + 0.393\tau_a^{1.045})}. \quad (22)$$

For an infinite slab geometry and photons injected isotropically at midplane:

$$\frac{1}{P} = 0.992 \frac{1 + 123.2\tau_a}{1 + 124.9\tau_a} \exp[0.250\tau_a^{1.211} + 0.401\tau_d^{0.602 + (0.748\tau_a - 0.0464\tau_a^2)^{0.813}}]. \quad (23)$$

These expressions are general and can be applied to any situation where both absorption and scattering are important. For the situation considered in this work, the scattering τ_d and absorption τ_a optical depths depend on the type of radiation considered (see section 4):

- For the Comptonised component: $\tau_d = \tau_T$ and $\tau_a = \tau_B$
- For the reflected component: $\tau_d = a_R \tau_B$, $\tau_a = \tau_T + (1 - a_R) \tau_B$
- For the soft component: $\tau_d = \tau_B$, $\tau_a = \tau_T$

Note that we neglect the relativistic effects due to the reduction of the Klein-Nishina cross section at high energies.